Adsorption of acetone and cyclohexane onto CO_2 activated hydrochars

Xueyang Zhang [a, b, c], Wei Xiang [a, b], Bing Wang [d], June Fang [b], Weixin Zou [c], Feng He [e], Yuncong Li [f], Daniel C.W. Tsang [g], Yong Sik Ok [h], Bin Gao [b, *]

[a] School of Environmental Engineering, Jiangsu Key Laboratory of Industrial Pollution Control and Resource Reuse, Xuzhou University of Technology, Xuzhou, 221018, PR China
[b] Department of Agricultural and Biological Engineering, University of Florida, Gainesville, FL, 32611, USA
[c] Jiangsu Key Laboratory of Vehicle Emissions Control, Center of Modern Analysis, Nanjing University, Nanjing, 210093, PR China
[d] State Key Laboratory of Environmental Geochemistry, Institute of Geochemistry Chinese Academy of Sciences, Guiyang, 550081, PR China
[e] College of Environment, Zhejiang University of Technology, Hangzhou, 310014, China
[f] Tropical Research and Education Center, University of Florida, Homestead, FL, 33031, USA
[g] Department of Civil and Environmental Engineering, The Hong Kong Polytechnic University, Hung Hom, Kowloon, Hong Kong, China
[h] Korea Biochar Research Center & Division of Environmental Science and Ecological Engineering, Korea University, Seoul, 02841, Republic of Korea

H I G H L I G H T S

- Adsorption of acetone and cyclohexane onto pristine hydrochars was low (13.24–24.64 mg/g).
- CO_2 treatment increased VOC adsorption onto activated hydrochars (39.42–121.74 mg/g).
- Narrow hydrochar pore size and high VOC boiling point restrained the desorption .
- CO_2-activated hydrochars showed good reusability after five continuous cycles.

G R A P H I C A L   A B S T R A C T
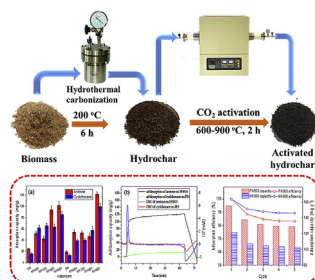
A R T I C L E   I N F O

A B S T R A C T

Most of the volatile organic compounds (VOCs) are toxic and harmful to human health and environment. In this study, hydrochars activated with CO_2 were applied to remove VOCs. Two typical VOCs, acetone and cyclohexane, were used as the 'model' adsorbates to evaluate hydrochars' performance. Specific surface areas of pristine hydrochars were small (<8 m^2/g), whereas activated hydrochars showed much higher values (up to 1308 m^2/g). As a result, the adsorption of VOCs onto the pristine hydrochars (13.24 –24.64 mg/g) was lower than that of the activated ones (39.42–121.74 mg/g). The adsorption of the two VOCs onto the hydrochars was exothermal. In addition, there were significant correlations ($R^2 > 0.91$) between the VOC removal and hydrochars' specific surface area. These results suggest that the governing mechanism was mainly physical adsorption. Increasing experimental temperature (80–139 °C) desorbed the VOCs from the hydrochars. Due to its higher boiling point, cyclohexane desorption required a higher temperature than acetone desorption. The reusability of the activated hydrochars to the two VOCs was confirmed by five continuous adsorption-desorption cycles. The overall results indicated that hydrochars, particularly after CO_2 activation, are sufficient for VOC abatement.

© 2019 Elsevier Ltd. All rights reserved.

* Corresponding author.
E-mail address: bg55@ufl.edu (B. Gao).

1. Introduction

Biochar is a porous black carbon produced from biomass by thermal processes with absence or limited supply of oxygen (Xiong et al., 2017; Zhang et al., 2017a). The feedstock materials of biochar are usually from the waste and residues of plants or animals (Igalavithana et al., 2017), and municipal waste, such as agricultural and forestry residues, sewage sludge, manures, and organic wastes (Wang et al., 2018; Yoo et al., 2018; Zheng et al., 2019). The most common method of biochar production is pyrolysis, which however is not applicable to high moisture feedstock (Ahmad et al., 2014; Cao et al., 2019). To get rid of the high moisture of the feedstock, it requires high energy for vaporization, which is the main drawback of pyrolysis (Kambo and Dutta, 2015; Fang et al., 2018). Under this situation, hydrothermal carbonization (HTC) technique has been considered to be a suitable method for the conversion of high moisture biomass (Fang et al., 2018). The char created by HTC is named as hydrochar to be distinguished from biochar produced from pyrolysis (Fang et al., 2015; Cao et al., 2017, 2019).

HTC is usually operated between 120 °C and 300 °C (Mohan et al., 2014; Cha et al., 2016; Fang et al., 2016). During HTC, the physical structure of biomass can be changed by chemical reactions such as hydrolysis, dehydration, decarboxylation, aromatization and condensation (Funke and Ziegler, 2010). Among them, hydrolysis is the primary reaction and need less activation energy than pyrolysis (Libra et al., 2011; Zhang et al., 2019b). Because of its low operation temperature, hydrochar normally has higher yield than biochar (Melo et al., 2019; Zhu et al., 2019).

Based on afore mentioned advantages, hydrochar has been suggested to be a value-added multifunctional materials for various applications, especially in environmental remediation and restorations (Tag et al., 2017; Wang et al., 2018; Melo et al., 2019). For example, hydrochars and their derivatives have been applied to remove various contaminants including methylene blue ($C_{16}H_{18}ClN_3S$), copper (Cu^{2+}), and lead (Pb^{2+}) from wastewater (Xue et al., 2012; Fang et al., 2016). The characteristics and potential applications of hydrochar are related to the reaction temperature, holding time, and other factors (Choe et al., 2019; Yao and Ma, 2019). With the increase of temperature and holding time, hydrochar contains more acidic surface functional groups and larger porous structure, which can increase its adsorption ability to environmental pollutants (Melo et al., 2017; Zhou et al., 2017; Saha et al., 2019).

Hydrochar benefits by the low energy consumption and high production rate, however, both of its pore volume (PV) and specific surface area (SSA) are small (Sun et al., 2014), which may limit its applications as an effective adsorbent. Therefore, it is necessary to modify hydrochar to increase its adsorption ability (Rajapaksha et al., 2016). Acid and alkali are common modifying agents which can effectively enhance the SSA and PV of hydrochar (Zhang et al., 2019a). Other modification technologies, such as magnetic, ball milling, and oxidation treatments, can also be applied to improve hydrochar's adsorptive properties (Rajapaksha et al., 2016; Usman et al., 2016; Lyu et al., 2018). CO_2 activation can create pore structures on carbon materials to expend SA (Lee et al., 2017; Yang et al., 2018), thus it is one of the most popular activation methods for activated carbon production. Nevertheless, little research has been conducted to evaluate CO_2 modified hydrochars.

Volatile organic compounds (VOCs) are harmful pollutants in the atmosphere which threaten the human health and environment because they are toxic and often carcinogenic, and can cause photochemical smog and stratospheric ozone depletion (Khan et al., 2019; Zou et al., 2019). Among numerous VOC elimination techniques, adsorption has been applied extensively because it can remove and recover VOCs effectively at a low cost (Zhang et al., 2017a; Khan et al., 2019). The application of biochar on VOC adsorption has been explored in the latest literature. Biochars produced from rice husk (Li et al., 2016; Fu et al., 2019), swine manure (Hwang et al., 2018), peanut shell (Zhang et al., 2017b), municipal solid waste (Jayawardhana et al., 2019), pinecone (Yi et al., 2018), and their derivatives have been used to adsorb VOCs. However, limited research focused on the VOCs removal by activated hydrochars (Zhang et al., 2019a).

The overarching goal of this study is to evaluate the VOC removal ability of hydrochars, particularly the ones activated by CO_2. Adsorption experiments of acetone and cyclohexane onto the pristine and modified hydrochars produced from peanut shell and hickory wood chips were conducted with the specific objectives of: (1) assess the applicability of hydrochar as an adsorbent for VOC removal, (2) determine the effect of CO_2 activation on the adsorption ability of hydrochar to VOCs, and (3) expound the adsorptive mechanisms of hydrochars toward VOCs.

2. Materials and methods

2.1. Materials

Pristine hydrochars were produced according to the protocols in the literature (Fang et al., 2015). In brief, milled hickory wood chips and peanut shell of sizes of 0.5−1 mm were putted into a HTC reactor. Whereafter, the feedstock was submerged in distilled water. After sealed, the reactor was heated on a hotplate at 200 °C for 6 h. The obtained hydrochar was rinsed by tap water for 10 min and distilled water for 5 min, followed by drying in the electricity heat drum wind drying oven at 70 °C overnight. The obtained products were labeled as HH and PH for hickory wood chips and peanut shell hydrochar, respectively.

The CO_2 activation procedures was performed according to the literature (Fang et al., 2016). Briefly, part of the obtained hydrochar was added into a quartz tube furnace, and activated under the atmosphere of 150 mL/min CO_2. The activation was persistent for 2 h at the temperature of 600, 700, 800, and 900 °C. The obtained CO_2 activated hydrochars were abbreviated as HH600, HH700, HH800, and HH900; and PH600, PH700, PH800, and PH900 with letters for hydrochar and numbers for activation temperature. The basic properties of the adsorbents applied in this work are listed in Table S1, which were characterized elsewhere (Fang et al., 2016). Acetone (polar VOC) and cyclohexane (nonpolar VOC) were chemically pure and used in the adsorption experiment as the VOCs.

2.2. VOC adsorption and desorption experiments

Adsorption experiments were carried out using the gravimetric analysis method developed in previous studies (Zhang et al., 2017b, 2019a). Approximately 10 mg of the adsorbent was added to a 70 μL aluminum oxide crucible and flushed at 110 °C for 1 h under the atmosphere of nitrogen. Then the inlet gas would change to 50 mL/min VOC vapor since it was cooled to the testing temperature (i.e., 20, 40, or 60 °C). The adsorption persisted for 1 h. Desorption was carried out by raising the adsorption temperature to 150 °C with the heating rate of 10 °C/min. Duplicated measurements were taken to get the average of each test.

2.3. Adsorption kinetics

The kinetic data were described using pseudo-first and pseudo-second order models:

$$q_t = q_e \left(1 - e^{-k_1 t}\right) \qquad (1)$$

$$q_t = \frac{t \cdot k_2 \cdot q_e^2}{1 + q_e \cdot t \cdot k_2} \qquad (2)$$

where q_e and q_t are the quantities of VOC sorbed at equilibrium and time t, respectively; and k_1 and k_2 are the first-order and second-order adsorption rate constants, respectively.

3. Results and discussion

3.1. Adsorbent properties

The basic characteristics of hydrochars vary with the feedstock type and pyrolysis temperature (Table S1). The effects of feedstock type on biochar and hydrochar properties have been attributed to the different compositions and proportions of cellulose, hemicellulose, and lignin in the feedstock biomass (Sun et al., 2014). Compared with cellulose and hemicellulose, lignin is more stable and resistant to the decomposition of liquid and gaseous fractions (Fang et al., 2015). Comparing the SSA of hydrochars produced at the same condition, most of the hickory wood chips derived hydrochars had higher SSA (8 m^2/g for pristine hydrochar and 453–667 m^2/g for modified ones) than the corresponding peanut shell hydrochars (7 m^2/g for pristine hydrochar and 353–488 m^2/g for modified ones). Among all the samples, hydrochars activated at 900 °C were exceptional. The SSA of HH900 was 928 m^2/g, which is smaller than that of PH900 (1308 m^2/g). The SSA of the activated hydrochars increased with elevating the treatment temperature. When the temperature elevated from 600 to 900 °C, the SSA of both HH and PH increased 1–3 times.

Different from the SSA, the PV of the activated hydrochars did not show obvious relationship with the activation temperature. HH had the largest BJH-PV of 0.121 mL/g. After CO$_2$ activation, PH700 and PH900 had the largest BJH-PV of 0.114 mL/g. Increasing the activation temperature may have opposite affects: 1) Pore volume and pore diameter may be enlarged as the walls between adjacent pores being fused; however, this will decrease microporosity. 2) pore volume may decrease due to the collapse and filling of the pore.

As the activation temperature elevated, the hydrochar C content increased from 68.7% to 90.5%, and from 70.6% to 88.7% for HH and PH based hydrochars, respectively; while the H content decreased (from 5.3% to 0.2%, and from 6.0% to 1.2% for HH and PH based hydrochars, respectively). The results reflect the release of organic compounds from hydrochars during activation. The volatization and conversion of organic phase of the pristine hydrochars may induce pore volume enlargement, while the C skeleton would retain the rudimentary porosity and original structure (Zhao et al., 2014). Changes in morphology and structures of hydrochars after activation can affect their adsorptive properties significantly, which will be investigated in the subsequent sections.

3.2. Adsorption rates

The pristine hydrochars had low VOC adsorption with capacities of 13.24–24.64 mg/g (Fig. 1a), which are comparable to those of biochars derived from the same feedstock, especially the low temperature ones. Zhang et al. found the acetone and cyclohexane adsorption capacities of 300 °C hickory wood biochar were 7.06 mg/g and 7.44 mg/g, respectively, while those of 600 °C hickory wood biochar were 39.73 mg/g and 48.25 mg/g, respectively (Zhang et al., 2017b). In this work, HH had higher adsorption capacities for acetone and cyclohexane than HP, reflecting the importance of feedstock to hydrochar's sorptive properties.

After CO$_2$ activation, the adsorption capacities of the hydrochars increased dramatically into 39.42–121.74 mg/g (Fig. 1a), much higher than those of biochars derived from the same feedstock. Generally, the amount of VOC adsorbed on activated hydrochar increased with elevating the activation temperature. Similar phenomenon have been observed in the investigations of SO$_2$, dye (C$_{16}$H$_{18}$ClN$_3$S), and heavy metal (Pb^{2+}, Cu^{2+}, and Cd^{2+}) adsorption onto CO$_2$ activated hydrochars (Fang et al., 2016; Shao et al., 2018). Activated hydrochar produced at higher temperature had the higher adsorption rate, which may be ascribed to the larger SSA and suitable pore structure, as shown in the previous section.

The typical sorption and differential scanning calorimetry (DSC) curves of VOCs on hydrochars are presented in Fig. 1b, in which acetone adsorption onto PH900 (the highest adsorption) and cyclohexane adsorption onto PH (the lowest adsorption) were chosen as representatives. Both curves showed obvious VOC adsorption, accompanied with notable exothermic peaks. Besides, obvious weight loss was observed during the desorption phase, when the temperature was raised from 20 °C to 150 °C. Meanwhile, the endothermic peaks were obvious, corresponding to the increase of temperature needed for the VOC desorption.
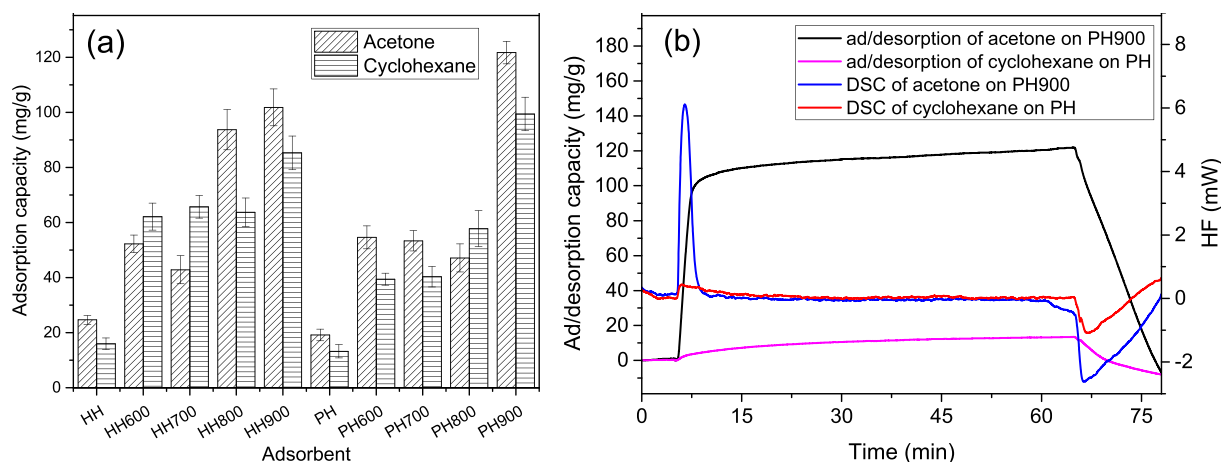

Fig. 1. (a) Adsorption rates of acetone and cyclohexane onto hydrochars at 20 °C, and (b) typical adsorption and desorption and DSC curves of VOCs on hydrochars.

3.3. Adsorption kinetics and mechanisms

The 1st and 2nd order models are often employed to simulate VOC adsorption process. The optimal model parameters in this work are presented in Table 1. The 2nd order model was superior than 1st order model for polar acetone adsorption kinetics; while it was opposite for the nonpolar cyclohexane adsorption kinetics. This result suggests that the adsorption of different polarity VOC onto the hydrochars could be controlled by different mechanisms.

VOC adsorption onto carbonaceous adsorbents are mainly controlled by mechanisms related to Van der Waals interaction, π-π bond, hydrophobic effect, hydrogen bond, and covalent and electrostatic interactions (Zhang et al., 2017a). Among them, Van der Waals interaction is one of the most important physical adsorption mechanisms for VOCs on porous adsorbents. The attractive forces between VOC molecules and carbon material can be affected by polarity. As shown in Fig. 2, for the polar molecules (e.g., acetone), there are three types of intermolecular forces, namely induced dipole-induced dipole, dipole-induced dipole, and dipole-dipole forces. Whereas there is only induced dipole-induced

dipole force for nonpolar molecules (e.g., cyclohexane). The reinforced molecular forces of dipole-dipole and induced dipole-dipole on polar molecules are comparable to the medium-strength hydrogen bond, which are stronger than the induced dipole-induced dipole force (Wade and Simek, 2016). Thus, polar acetone showed higher adsorption than nonpolar cyclohexane on the hydrochars with polar surface.

In addition to the Van der Waals forces, π-π dispersion interaction is another important mechanism of VOC adsorption. Most of the carbon atoms in carbonaceous materials have the π electron orbit, which can be bound with VOC molecules with π electrons (such as acetone) to form π-π dispersion interaction with face-to-face or offset face-to-face orientations (Pan and Xing, 2008; Qu et al., 2009). However, all the six carbon atoms of cyclohexane are hybridized by sp^3 and there is no extra orbital available to form the π bond. Therefore, cyclohexane cannot be adsorbed onto the hydrochars via π-π dispersion interaction.

Large specific surface area is important to VOC adsorption through Van der Waals interaction and π-π bond. The relationships between SSA of hydrochars and their acetone and cyclohexane

Table 1
Parameters of adsorption dynamic models used for modeling acetone and cyclohexane adsorption onto hydrochars at 20 °C.

| Adsorbate	Model	1st order model			2nd order model			q_e, exp(mg/g)
	Parameters	q_e(mg/g)	k_1(1/min)	R^2	q_e(mg/g)	k_2(g/mg·min)	R^2	
Acetone	HH	25.21	0.077	0.997	31.45	0.0025	0.984	24.64
	HH600	50.38	0.627	0.836	52.32	0.0221	0.990	52.24
	HH700	40.99	0.517	0.864	42.89	0.0212	0.976	42.84
	HH800	90.02	0.353	0.937	95.62	0.0062	0.974	93.70
	HH900	99.62	0.581	0.908	103.70	0.0100	0.847	101.81
	PH	17.96	0.214	0.846	19.56	0.0175	0.976	19.19
	PH600	51.98	0.249	0.915	56.17	0.0071	0.995	54.61
	PH700	49.87	0.186	0.870	54.85	0.0052	0.980	53.35
	PH800	44.39	0.204	0.813	48.43	0.0068	0.964	47.12
	PH900	116.40	0.488	0.900	122.21	0.0067	0.886	121.74
Cyclohexane	HH	15.52	0.142	0.942	17.45	0.0117	0.994	15.98
	HH600	62.48	0.102	0.999	73.97	0.0016	0.987	62.12
	HH700	66.40	0.087	0.999	80.82	0.0012	0.987	65.69
	HH800	62.54	0.091	0.993	74.96	0.0014	0.999	63.71
	HH900	84.36	0.828	0.728	86.88	0.0186	0.978	85.29
	PH	12.72	0.133	0.924	14.34	0.0134	0.983	13.24
	PH600	38.52	0.067	0.979	48.21	0.0015	0.996	39.42
	PH700	39.88	0.053	0.952	51.39	0.0010	0.979	40.32
	PH800	55.64	0.077	0.973	68.03	0.0013	0.995	57.76
	PH900	95.12	0.251	0.899	102.45	0.0041	0.991	99.41
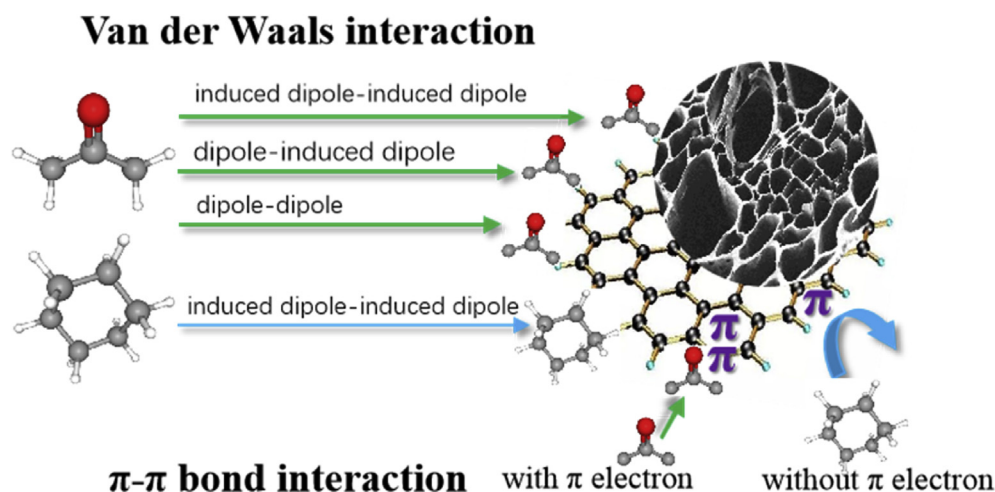
Fig. 2. Adsorption mechanisms of acetone and cyclohexane onto activated hydrochar.
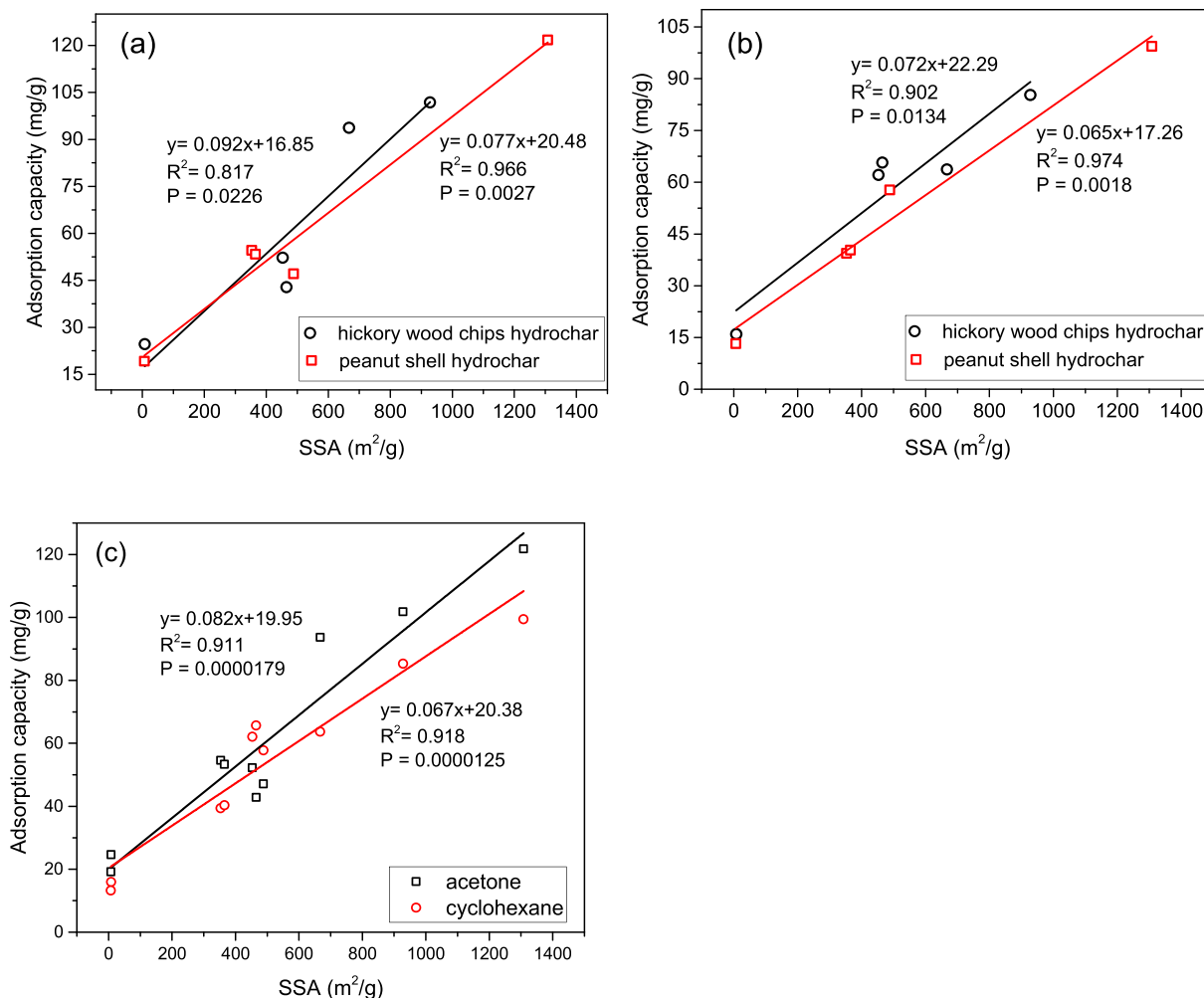
Fig. 3. Relationships between SSA and VOC adsorption capacity of hydrochars: (a) acetone on hydrochars from different feedstock, (b) cyclohexane on hydrochars from different feedstock, and (c) different VOCs on all hydrochars.

adsorption capacity are analyzed (Fig. 3). The adsorption of polar acetone and non-polar cyclohexane was significantly correlated with SSA with the R^2 ranging 0.911−0.918 ($p < 0.01$). This suggests that physical adsorption was the prevailing mechanism of VOC adsorption onto the hydrochars. The importance of surface area to VOC removal by carbonaceous adsorbents has been recognized in the literature, such as benzene, methylbenzene and xylene onto activated carbon fibers (Das et al., 2004); hexyl hydride and chlorylene onto carbon nanotube (Shih and Li, 2008); and dimethyl ketone, hexamethylene, and methylbenzene onto biochars (Zhang et al., 2017b).

Pore volume is another important factor to VOC adsorption onto carbonaceous adsorbents. The relationships between BJH pore volume of hydrochars and their acetone and cyclohexane adsorption capacities are presented in Fig. 4. Nevertheless, the correlation between BJH pore volume and VOC adsorption rate was poor, with the R^2 values of 0.419−0.786 ($p < 0.238$).

3.4. Temperature effect

VOC adsorption onto poriferous adsorbents is mainly controlled by physical exothermic interaction. The adsorption of acetone on the ten hydrochars decreased with elevating adsorption temperature (Fig. 5a). Increasing the temperature from 20 °C to 40 °C and

from 20 °C to 60 °C, acetone adsorption decreased by 9%−61% and 20%−74%, respectively. The temperature effect was the most dramatic to hydrochars activated at high temperature. For example, acetone adsorption onto HH900 and PH900 decreased 61% and 74%, respectively, with the increase of adsorption temperature. In comparison, variation of temperature showed a different effect on cyclohexane adsorption. For most of the hydrochars except PH800 and PH900, the highest cyclohexane adsorption was observed at 40 °C (Fig. 5b). When the temperature increased to 60 °C, VOC adsorption on the hydrochars decreased by 9%−64%. Previous studies have reported that increasing experimental temperature can also reduce the removal of CH_2Cl_2 and CH_3I onto activated carbon as well as acetone onto biochar (Qian et al., 2015; Zhang et al., 2017b).

It is well recognized that elevating the temperature can decrease the adsorption if it is an exothermic process. Yet when intrapore diffusion is a rate-limiting step, however, high adsorption temperature can facilitate the transfer of VOCs into the pores of hydrochar adsorbents to promote the adsorption (Zhang et al., 2017a). Wang et al. (2015) studied the influence of temperature on VOC sorption and found that the sorption rate coefficient of benzene, hexamethylene, and hexyl hydride adsorption onto ordered mesoporous carbons at 45 °C were higher than those at 35 °C or 25 °C. In this study, acetone has small kinetic diameter of
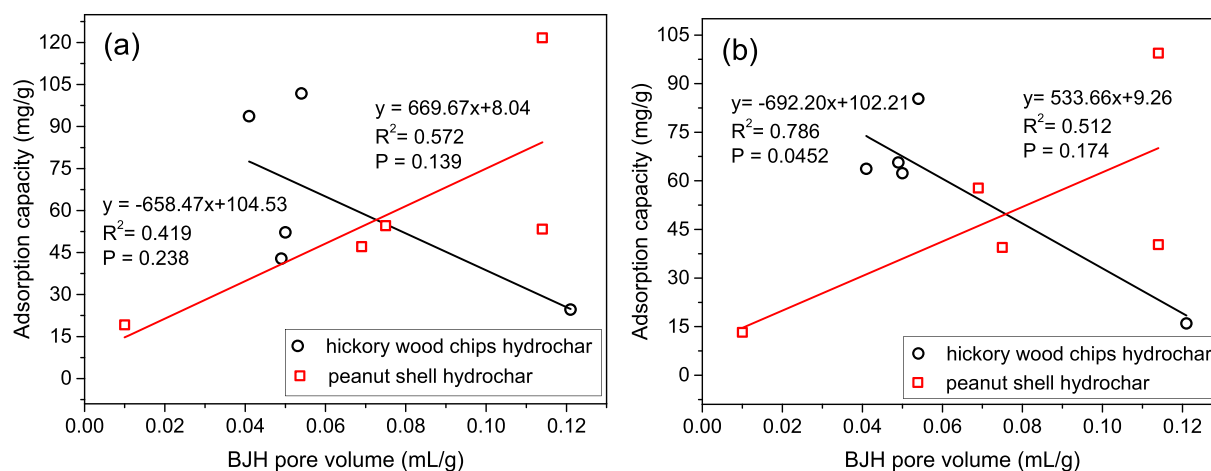
Fig. 4. Relationships between BJH pore volume and acetone (a) and cyclohexane (b) adsorption capacity.
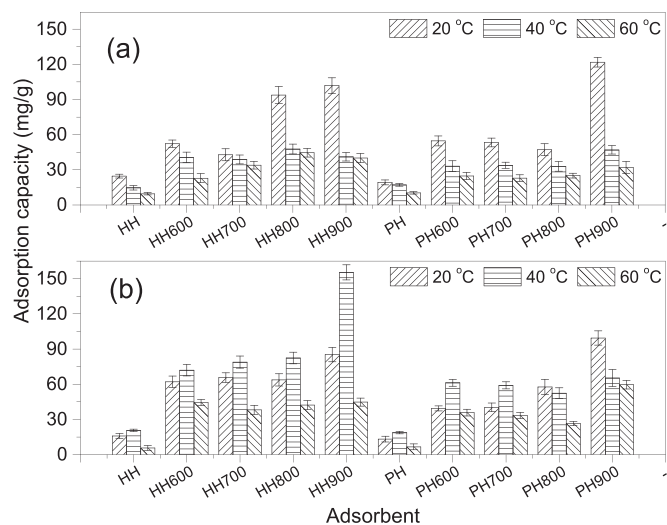

Fig. 5. Adsorption capacities of hydrochars to acetone (a) and cyclohexane (b) at 20 °C, 40 °C, and 60 °C.

0.46 nm and is easy diffused into the pores. While the size of cyclohexane is larger (kinetic diameter of 0.60 nm) and a slightly higher adsorption temperature (40 °C) thus may benefit its adsorption onto the hydrochars.

3.5. Desorption and reusability

All the adsorbed acetone could be desorbed from the hydrochars at the temperature of 78−114 °C (Fig. 6). The effective desorption temperature varied with the type of the adsorbents. Generally, the required desorption temperature was higher for hydrochars activated at higher temperature. For example, PH and HH had the lowest desorption temperatures of 80 °C and 88 °C, respectively; while PH800 and HH800 had the highest desorption temperature of 114 °C and 109 °C, respectively. Cyclohexane on the hydrochars showed similar desorption behavior to acetone, but its desorption temperature was slightly higher (71−139 °C). Besides, cyclohexane on HH900 could not be entirely desorbed with 17.1% retained even at 150 °C.

Because hydrochars activated at higher temperature possess larger SSA and more micropores (Table S1), VOCs adsorbed on these adsorbents thus may require more energy (i.e., higher desorption temperature) to escape from carbon surface and the micropore structure (Wang et al., 2009; Zhang et al., 2017a). Lashak et al. (Lashaki et al., 2012) reported similar results that high desorption temperature can increase VOC regeneration efficiency of beaded activated carbon with narrow micropores (0.5−0.7 nm).

As for the result that the desorption temperature of cyclohexane was higher than that of acetone, it may be ascribed to the different boiling points of the two VOCs. Previous studies have indicated that VOCs with higher boiling points also have stronger affinity for carbonaceous adsorbents (Lashaki et al., 2012; Shah et al., 2014; Son et al., 2016; Zhang et al., 2019a). The boiling point of cyclohexane is 80.74 °C, which is higher than that of acetone (56.53 °C). As a result, cyclohexane is expected to require higher temperature than acetone to be desorbed from the hydrochars.

Reusability tests of selected hydrochars to acetone and cyclohexane were carried out. Based on the best adsorption performance of each VOC, acetone adsorption on HH900 at 20 °C and cyclohexane adsorption on PH900 at 40 °C were chosen to determine the reusability. As shown in Fig. 7, after five successive cycles, the adsorption capacity of acetone on HH900 only decreased slightly from 121.74 mg/g to 102.84 mg/g with nearly 90% of the adsorption capacity at the end of the tests. As for the adsorption of cyclohexane on PH900, slightly more reduction of the adsorption capacity was observed. After five successive reuses, the adsorption capacity decreased from 155.41 mg/g to 128.97 mg/g with 83.30% capacity remaining. More cyclohexane was retained in the hydrochar than acetone during the regeneration (i.e., incomplete desorption), which can be ascribed to its higher boiling point and stronger adhesion to the hydrochar.

4. Conclusions

In this work, pristine and CO_2-activated hydrochars were used to adsorb two typical VOCs (polar acetone and nonpolar cyclohexane). After CO_2 activation, the SSA of hydrochars increased significantly from 8 m^2/g to 1308 m^2/g. Their VOC adsorptive capacities increased from 13.24 to 24.64 mg/g to 39.42−121.74 mg/g accordingly. The significant linear correlation between VOC adsorption capacities and specific surface areas, together with the notable adsorption exothermal peaks of DSC curves suggest that physical adsorption was the main mechanism of VOC adsorption on the hydrochars. The desorption of VOCs from hydrochars was
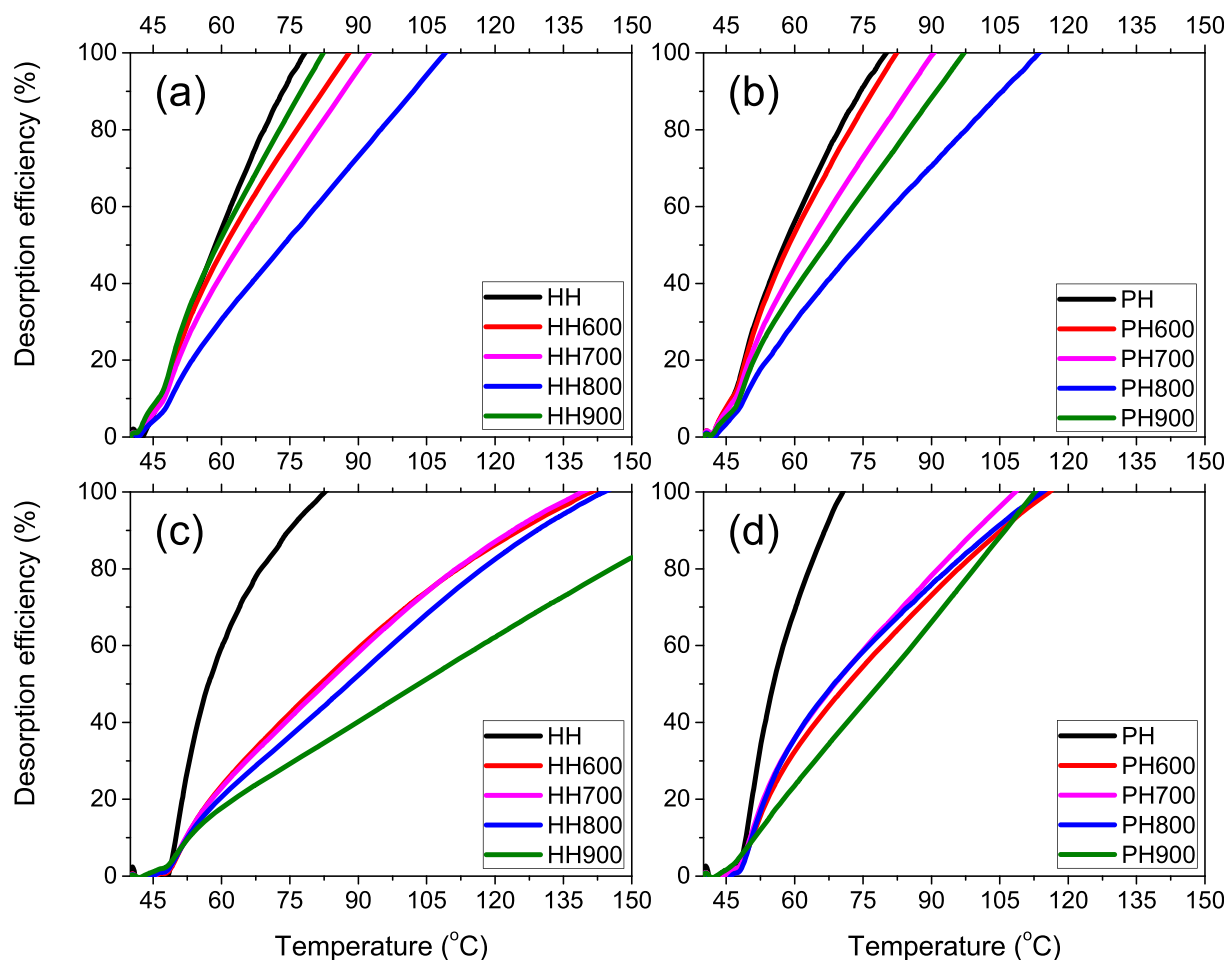
Fig. 6. Desorption efficiency of acetone on hydrochars produced from hickory wood chips (a) and peanut shell (b); and cyclohexane on hydrochars produced from hickory wood chips (c) and peanut shell (d).
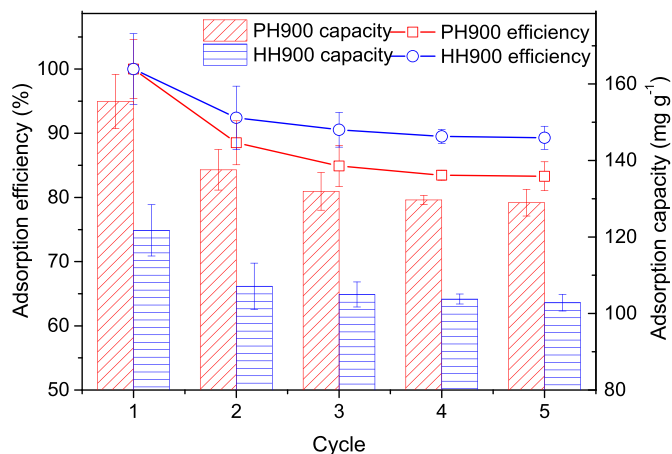

Fig. 7. Reuse experiments of cyclohexane on PH900 at 40 °C and acetone on HH900 at 20 °C.

affected by hydrochar pore size and VOC boiling point. VOCs on the hydrochars could be desorbed by raising the experimental temperature. Narrow pore size and high boiling point may restrain VOC desorption and thus require high desorption temperature. CO_2-activated hydrochars showed good reusability after five cycles,

suggesting they can be used as an effective VOC adsorbent.

Author contribution statement

Xueyang Zhang: Conceptualization, Methodology, Formal analysis, Investigation,Writing- Original draft preparation. **Wei Xiang, Bing Wang, June Fang, & Weixin Zou**: Methodology, Formal analysis, Investigation, Writing - Review & Editing. **Feng He, Yuncong Li, Daniel C.W. Tsang, & Yong Sik Ok:** Writing - Review & Editing.**Bin Gao:** Conceptualization, Methodology, Formal analysis, Writing - Review &Editing.

Acknowledgments

Appendix A. Supplementary data

Supplementary data to this article can be found online at https://doi.org/10.1016/j.chemosphere.2019.125664.

References

Ahmad, M., Rajapaksha, A.U., Lim, J.E., Zhang, M., Bolan, N., Mohan, D., Vithanage, M., Lee, S.S., Ok, Y.S., 2014. Biochar as a sorbent for contaminant management in soil and water: a review. Chemosphere 99, 19–33.

Cao, L., Yu, I.K.M., Cho, D.-W., Wang, D., Tsang, D.C.W., Zhang, S., Ding, S., Wang, L., Ok, Y.S., 2019. Microwave-assisted low-temperature hydrothermal treatment of red seaweed (Gracilaria lemaneiformis) for production of levulinic acid and algae hydrochar. Bioresour. Technol. 273, 251–258.

Cao, L., Zhang, C., Chen, H., Tsang, D.C.W., Luo, G., Zhang, S., Chen, J., 2017. Hydro-thermal liquefaction of agricultural and forestry wastes: state-of-the-art review and future prospects. Bioresour. Technol. 245, 1184–1193.

Cha, J.S., Park, S.H., Jung, S.-C., Ryu, C., Jeon, J.-K., Shin, M.-C., Park, Y.-K., 2016. Production and utilization of biochar: a review. J. Ind. Eng. Chem. 40, 1–15.

Choe, U., Mustafa, A.M., Lin, H., Xu, J., Sheng, K., 2019. Effect of bamboo hydrochar on anaerobic digestion of fish processing waste for biogas production. Bioresour. Technol. 283, 340–349.

Das, D., Gaur, V., Verma, N., 2004. Removal of volatile organic compound by acti-vated carbon fiber. Carbon 42, 2949–2962.

Fang, J., Gao, B., Chen, J., Zimmerman, A.R., 2015. Hydrochars derived from plant biomass under various conditions: characterization and potential applications and impacts. Chem. Eng. J. 267, 253–259.

Fang, J., Gao, B., Zimmerman, A.R., Ro, K.S., Chen, J., 2016. Physically (CO₂) activated hydrochars from hickory and peanut hull: preparation, characterization, and sorption of methylene blue, lead, copper, and cadmium. RSC Adv. 6, 24906–24911.

Fang, J., Zhan, L., Ok, Y.S., Gao, B., 2018. Minireview of potential applications of hydrochar derived from hydrothermal carbonization of biomass. J. Ind. Eng. Chem. 57, 15–21.

Fu, Y., Shen, Y., Zhang, Z., Ge, X., Chen, M., 2019. Activated bio-chars derived from rice husk via one- and two-step KOH-catalyzed pyrolysis for phenol adsorption. Sci. Total Environ. 646, 1567–1577.

Funke, A., Ziegler, F., 2010. Hydrothermal Carbonization of Biomass: A Literature Survey Focusing on its Technical Application and Prospects.

Hwang, O., Lee, S.-R., Cho, S., Ro, K.S., Spiehs, M., Woodbury, B., Silva, P.J., Han, D.-W., Choi, H., Kim, K.-Y., Jung, M.-W., 2018. Efficacy of different biochars in removing odorous volatile organic compounds (VOCs) emitted from swine manure. ACS Sustain. Chem. Eng. 6, 14239–14247.

Igalavithana, A.D., Mandal, S., Niazi, N.K., Vithanage, M., Parikh, S.J., Mukome, F.N.D., Rizwan, M., Oleszczuk, P., Al-Wabel, M., Bolan, N., Tsang, D.C.W., Kim, K.-H., Ok, Y.S., 2017. Advances and future directions of biochar characterization methods and applications. Crit. Rev. Environ. Sci. Technol. 47, 2275–2330.

Jayawardhana, Y., Gunatilake, S.R., Mahatantila, K., Ginige, M.P., Vithanage, M., 2019. Sorptive removal of toluene and m-xylene by municipal solid waste biochar: simultaneous municipal solid waste management and remediation of volatile organic compounds. J. Environ. Manag. 238, 323–330.

Kambo, H.S., Dutta, A., 2015. A comparative review of biochar and hydrochar in terms of production, physico-chemical properties and applications. Renew. Sustain. Energy Rev. 45, 359–378.

Khan, A., Szulejko, J.E., Kim, K.-H., Sammadar, P., Lee, S.S., Yang, X., Ok, Y.S., 2019. A comparison of figure of merit (FOM) for various materials in adsorptive removal of benzene under ambient temperature and pressure. Environ. Res. 168, 96–108.

Lashaki, M.J., Fayaz, M., Wang, H., Hashisho, Z., Philips, J.H., Anderson, J.E., Nichols, M., 2012. Effect of adsorption and regeneration temperature on irre-versible adsorption of organic vapors on beaded activated carbon. Environ. Sci. Technol. 46, 4083–4090.

Lee, J., Yang, X., Cho, S.-H., Kim, J.-K., Lee, S.S., Tsang, D.C.W., Ok, Y.S., Kwon, E.E., 2017. Pyrolysis process of agricultural waste using CO₂ for waste management, energy recovery, and biochar fabrication. Appl. Energy 185, 214–222.

Li, M.-s., Wu, S.C., Peng, Y.-H., Shih, Y.-h., 2016. Adsorption of volatile organic vapors by activated carbon derived from rice husk under various humidity conditions and its statistical evaluation by linear solvation energy relationships. Separ. Purif. Technol. 170, 102–108.

Libra, J.A., Ro, K.S., Kammann, C., Funke, A., Berge, N.D., Neubauer, Y., Titirici, M.M., Führer, C., Bens, O., Kern, J., 2011. Hydrothermal carbonization of biomass re-siduals: a comparative review of the chemistry, processes and applications of wet and dry pyrolysis. Biofuels 2, 71–106.

Lyu, H., Gao, B., He, F., Zimmerman, A.R., Ding, C., Huang, H., Tang, J., 2018. Effects of ball milling on the physicochemical and sorptive properties of biochar: exper-imental observations and governing mechanisms. Environ. Pollut. 233, 54–63.

Melo, T.M., Bottlinger, M., Schulz, E., Leandro, W.M., Botelho de Oliveira, S., Menezes de Aguiar Filho, A., El-Naggar, A., Bolan, N., Wang, H., Ok, Y.S., Rinklebe, J., 2019. Management of biosolids-derived hydrochar (Sewchar): effect on plant germination, and farmers' acceptance. J. Environ. Manag. 237, 200–214.

Melo, T.M., Bottlinger, M., Schulz, E., Leandro, W.M., de Aguiar Filho, A.M., Ok, Y.S., Rinklebe, J., 2017. Effect of biosolid hydrochar on toxicity to earthworms and brine shrimp. Environ. Geochem. Health 39, 1351–1364.

Mohan, D., Sarswat, A., Ok, Y.S., Pittman Jr., C.U., 2014. Organic and inorganic con-taminants removal from water with biochar, a renewable, low cost and sus-tainable adsorbent − a critical review. Bioresour. Technol. 160, 191–202.

Pan, B., Xing, B., 2008. Adsorption mechanisms of organic chemicals on carbon nanotubes. Environ. Sci. Technol. 42, 9005–9013.

Qian, Q., Gong, C., Zhang, Z., Yuan, G., 2015. Removal of VOCs by activated carbon microspheres derived from polymer: a comparative study. Adsorption 21, 333–341.

Qu, F., Zhu, L., Yang, K., 2009. Adsorption behaviors of volatile organic compounds (VOCs) on porous clay heterostructures (PCH). J. Hazard Mater. 170, 7–12.

Rajapaksha, A.U., Chen, S.S., Tsang, D.C.W., Zhang, M., Vithanage, M., Mandal, S., Gao, B., Bolan, N.S., Ok, Y.S., 2016. Engineered/designer biochar for contaminant removal/immobilization from soil and water: potential and implication of biochar modification. Chemosphere 148, 276–291.

Saha, N., Saba, A., Reza, M.T., 2019. Effect of hydrothermal carbonization tempera-ture on pH, dissociation constants, and acidic functional groups on hydrochar from cellulose and wood. J. Anal. Appl. Pyrolysis 137, 138–145.

Shah, I.K., Pre, P., Alappat, B.J., 2014. Effect of thermal regeneration of spent acti-vated carbon on volatile organic compound adsorption performances. J. Taiwan Inst. of Chemical Eng. 45, 1733–1738.

Shao, J., Zhang, J., Zhang, X., Feng, Y., Zhang, H., Zhang, S., Chen, H., 2018. Enhance SO₂ adsorption performance of biochar modified by CO₂ activation and amine impregnation. Fuel 224, 138–146.

Shih, Y.-h., Li, M.-s., 2008. Adsorption of selected volatile organic vapors on multiwall carbon nanotubes. J. Hazard Mater. 154, 21–28.

Son, H.K., Sivakumar, S., Rood, M.J., Kim, B.J., 2016. Electrothermal adsorption and desorption of volatile organic compounds on activated carbon fiber cloth. J. Hazard Mater. 301, 27–34.

Sun, Y., Gao, B., Yao, Y., Fang, J., Zhang, M., Zhou, Y., Chen, H., Yang, L., 2014. Effects of feedstock type, production method, and pyrolysis temperature on biochar and hydrochar properties. Chem. Eng. J. 240, 574–578.

Tag, A.T., Duman, G., Yanik, J., 2017. Influences of feedstock type and process vari-ables on hydrochar properties. Bioresour. Technol. 250, 337–344.

Usman, A.R.A., Ahmad, M., El-Mahrouky, M., Al-Omran, A., Ok, Y.S., Sallam, A.S., El-Naggar, A.H., Al-Wabel, M.I., 2016. Chemically modified biochar produced from conocarpus waste increases NO3 removal from aqueous solutions. Environ. Geochem. Health 38, 511–521.

Wade, L.G., Simek, J.W., 2016. Organic Chemistry, 9 th. Pearson Education.

Wang, G., Dou, B., Zhang, Z., Wang, J., Liu, H., Hao, Z., 2015. Adsorption of benzene, cyclohexane and hexane on ordered mesoporous carbon. J. Environ. Sci. 30, 65–73.

Wang, Q., Liang, X.Y., Zhang, R., Liu, C.J., Liu, X.J., Qiao, W.M., Zhan, L., Ling, L.C., 2009. Preparation of polystyrene-based activated carbon spheres and their adsorption of dibenzothiophene. N. Carbon Mater. 24, 55–60.

Wang, T., Zhai, Y., Zhu, Y., Li, C., Zeng, G., 2018. A review of the hydrothermal carbonization of biomass waste for hydrochar formation: process conditions, fundamentals, and physicochemical properties. Renew. Sustain. Energy Rev. 90, 223–247.

Xiong, X., Yu, I.K.M., Cao, L., Tsang, D.C.W., Zhang, S., Ok, Y.S., 2017. A review of biochar-based catalysts for chemical synthesis, biofuel production, and pollu-tion control. Bioresour. Technol. 246, 254–270.

Xue, Y., Gao, B., Yao, Y., Inyang, M., Zhang, M., Zimmerman, A.R., Ro, K.S., 2012. Hydrogen peroxide modification enhances the ability of biochar (hydrochar) produced from hydrothermal carbonization of peanut hull to remove aqueous heavy metals: batch and column tests. Chem. Eng. J. 200, 673–680.

Yang, X., Igalavithana, A.D., Oh, S.-E., Nam, H., Zhang, M., Wang, C.-H., Kwon, E.E., Tsang, D.C.W., Ok, Y.S., 2018. Characterization of bioenergy biochar and its utilization for metal/metalloid immobilization in contaminated soil. Sci. Total Environ. 640–641, 704–713.

Yao, Z.L., Ma, X.Q., 2019. Hydrothermal carbonization of Chinese fan palm. Bio-resour. Technol. 282, 28–36.

Yi, Y., Li, C., Zhao, L., Du, X., Gao, L., Chen, J., Zhai, Y., Zeng, G., 2018. The synthetic evaluation of CuO-MnOx-modified pinecone biochar for simultaneous removal formaldehyde and elemental mercury from simulated flue gas. Environ. Sci. Pollut. Res. Int. 25, 4761–4775.

Yoo, J.-C., Beiyuan, J., Wang, L., Tsang, D.C.W., Baek, K., Bolan, N.S., Ok, Y.S., Li, X.-D., 2018. A combination of ferric nitrate/EDDS-enhanced washing and sludge-derived biochar stabilization of metal-contaminated soils. Sci. Total Environ. 616–617, 572–582.

Zhang, X., Gao, B., Creamer, A.E., Cao, C., Li, Y., 2017a. Adsorption of VOCs onto engineered carbon materials: a review. J. Hazard Mater. 338, 102–123.

Zhang, X., Gao, B., Fang, J., Zou, W., Dong, L., Cao, C., Zhang, J., Li, Y., Wang, H., 2019a. Chemically activated hydrochar as an effective adsorbent for volatile organic compounds (VOCs). Chemosphere 218, 680–686.

Zhang, X., Gao, B., Zheng, Y., Hu, X., Creamer, A.E., Annable, M.D., Li, Y., 2017b. Biochar for volatile organic compound (VOC) removal: sorption performance and governing mechanisms. Bioresour. Technol. 245, 606–614.

Zhang, Z., Zhu, Z., Shen, B., Liu, L., 2019b. Insights into biochar and hydrochar production and applications: a review. Energy 171, 581–598.

Zhao, L., Zheng, W., Cao, X., 2014. Distribution and evolution of organic matter phases during biochar formation and their importance in carbon loss and pore structure. Chem. Eng. J. 250, 240–247.

Zheng, Y.P., Wang, B., Elise Wester, A., Chen, J., He, F., Chen, H., Gao, B., 2019. Reclaiming Phosphorus from Secondary Treated Municipal Wastewater with Engineered Biochar.

Zhou, N., Chen, H., Xi, J., Yao, D., Zhou, Z., Tian, Y., Lu, X., 2017. Biochars with excellent Pb(II) adsorption property produced from fresh and dehydrated

banana peels via hydrothermal carbonization. Bioresour. Technol. 232, 204—210.

Zhu, G.K., Yang, L., Gao, Y., Xu, J.Y., Chen, H.J., Zhu, Y.Z., Wang, Y.F., Liao, C.H., Lu, C., Zhu, C., 2019. Characterization and pelletization of cotton stalk hydrochar from

HTC and combustion kinetics of hydrochar pellets by TGA. Fuel 244, 479—491.

Zou, W., Gao, B., Ok, Y.S., Dong, L., 2019. Integrated adsorption and photocatalytic degradation of volatile organic compounds (VOCs) using carbon-based nano-composites: a critical review. Chemosphere 218, 845—859.